Structural evolution in the aging process of supercooled colloidal liquids

Takeshi Kawasaki[*] and Hajime Tanaka[†]

Institute of Industrial Science, University of Tokyo, 4-6-1 Komaba, Meguro-ku, Tokyo 153-8505, Japan
(Received 20 December 2013; revised manuscript received 27 May 2014; published 26 June 2014)

When a liquid is rapidly quenched to a temperature below the glass-transition point, it is driven out of equilibrium; it then slowly relaxes to a (quasi)equilibrium state. This slow relaxation process is called aging. By definition, any glasses are inevitably in the process of aging and actually slowly evolving with time. Thus the study of aging phenomena is of fundamental importance for understanding not only the nonequilibrium nature of the glass transition, but also the stability of glassy materials. Here we consider aging after a rather shallow quench, for which a system is still able to reach (metastable) equilibrium. By using polydisperse colloidal liquids as a model, we show the validity of dynamical scaling that there is only one relevant length scale not only for a quasiequilibrium supercooled state but also for a nonequilibrium process of aging, which is reminiscent of dynamical critical phenomena. Our finding indicates that the aging toward (metastable) equilibrium may be regarded as the growth process of critical-like fluctuations of static order associated with low-free-energy configurations, further suggesting that this ordering is the origin of cooperative slow dynamics in the systems studied. The generality of this statement for other glass-forming systems remains for a future study.

I. INTRODUCTION

The glass transition is usually regarded as a dynamical transition from an ergodic liquid to a nonergodic disordered solid state without any discontinuity [1,2]. However, the nonergodicity has to be defined on the basis of whether the structural relaxation takes place within the observation time or not. In this sense a glass-transition point is not uniquely defined but rather dependent upon the time scale of observation. One might argue that a glassy state should relax to a final (quasi)equilibrium state with a very long but finite relaxation time. For a deep quench, however, a system cannot relax to true equilibrium, but it can undergo increasingly slow partial relaxations, depending upon which internal degrees of freedom remain unfrozen [3]. For a shallow quench, on the other hand, aging can be regarded as the approach to (metastable) thermodynamic equilibrium. Here we restrict ourselves to the latter case. So hereafter aging means the relaxation process of a supercooled liquid toward its (metastable) equilibrium state.

During aging, the structural relaxation time τ_α increases with waiting time t_w with decreasing rate. Such behavior is observed not only in ordinary structural glasses [4–6] but also in so-called soft glassy materials [7–12]. Aging phenomena have also been studied intensively in spin-glass systems [13–15]. Unlike structural glasses, spin glasses have a well-defined phase transition of thermodynamic nature and a scaling argument based on the droplet picture has been developed [13–15]. On the basis of analogous behavior between spin and structural glasses, many interesting physical concepts such as effective temperature and an extended fluctuation-dissipation theorem have been proposed and lively discussed (see, e.g., [13,16]). The growth of the dynamical correlation length during aging was also found by numerical simulations [17,18], suggesting its connection to the slowing down of dynamics. However, since the very nature of the glass transition itself has remained elusive [2], there is no clear-cut understanding of the process of aging.

The most puzzling feature of the glass transition is that the structural relaxation time of a supercooled liquid increases drastically over many orders of magnitude upon cooling (or increasing density) toward the glass transition point, but without accompanying a noticeable change in the static structure seen by a two-body density correlator [e.g., the structure factor $S(q)$ and the radial distribution function $g(r)$] [19,20]. Since the finding of dynamic heterogeneity of a supercooled state (see [21–23] for two dimensions and [24–26] for three dimensions), the growing dynamical correlation and its link to slow dynamics have attracted considerable attention [27] and an analogy to critical phenomena was suggested [28]. However, the origin of dynamical heterogeneity is still elusive: For example, whether it is kinetic or static is a matter of debate [27].

The possible presence of growing static order has attracted considerable attention [1,2,29–38], although there are also different types of approaches such as a purely kinetic scenario and a mode-coupling approach (see, e.g., [1,2]). Candidates for such static order are icosahedral order [39,40], exotic amorphous order [41], and spatially extendable bond orientational order [32–37,42]. The usefulness of order agonistic static lengths such as a point-to-set length [43–45] is also actively discussed in connection to the random first-order transition scenario [1,2,41,46]. For weakly polydisperse colloidal liquids [33,35–37], driven granular matter [34], and spin liquids [32], we have recently shown that spatially extendable crystal-like bond orientational order is the origin of dynamic heterogeneity and slow glassy dynamics. We stress that this crystal-like bond orientational order should not be confused with crystalline order that accompanies translational order as well (see [33,35–37,42], particularly [37] for three dimensions): It is completely decoupled from the density field. We note that such orientational order arising from many-body correlations is difficult to detect by a two-body density correlator [47], which may be a reason why the importance

———————

[*]Present address: Laboratoire Charles Coulomb, UMR No. 5221, CNRS and Université Montpellier 2, Montpellier, France.
[†]tanaka@iis.u-tokyo.ac.jp

of structural ordering in a supercooled liquid had been overlooked [42,48]. The insufficiency of a description based on two-body correlations was also pointed out by Berthier and Tarjus [49] and by Coslovich [50]. We showed that such structural ordering can be revealed by using an appropriate structural order parameter for each type of system [35]. We also found [35,42,48] that this order parameter exhibits Ising-like criticality and argued that the slow dynamics may be explained by the activation-type critical dynamics [51–53]. Compared to ordinary critical phenomena, the range we can access is rather limited due to the much steeper slowing down, which makes the precise estimation of critical exponents difficult. Yet the Ising-like exponents of the diverging correlation length and susceptibility for two-dimensional (2D) and 3D polydisperse colloids, 2D driven granular matter, 3D Lennard-Jones polydisperse systems, and 2D spin liquids as well as the Ising-like (model A) order parameter dynamics [35] may be regarded as more than a coincidence. A theory supporting this scenario based on Ising criticality has recently been proposed by Langer [52,53]. In relation to the above, we note that similar local crystal-like order was also observed for 2D supermagnetic binary colloidal particles for both experiments and simulations [54]. In a supercooled liquid state, a system is widely believed to have a complex free-energy landscape with multibasins in the configuration space [55,56]. Then aging can be regarded as the process to seek a more stable state with lower free energy, which was recently confirmed for colloidal glasses [57]. According to our scenario, a state of lower free energy is linked to higher crystal-like bond orientational order for weakly polydisperse colloidal systems. This is natural for hard-sphere-like systems since the breakdown of local rotational symmetry allows for efficient local packing and thus increases the correlational entropy [42,48], i.e., lowers the free energy locally. This is particularly well established for 2D monodisperse hard-disk systems [58].

Here we study the slow relaxation process of polydisperse colloidal liquids as a function of the waiting time t_w (see Sec. II for the merits of using colloidal liquids) after a density jump [59] by means of Brownian dynamics simulations. We reveal that the aging toward metastable equilibrium can be regarded as the coarsening process of spatial fluctuations of glassy structural order, which is reminiscent of the dynamical scaling hypothesis of critical phenomena [60] that the growth of the correlation length $\xi(t_w)$ is the only relevant process and the whole time dependence enters only through $\xi(t_w)$ (see, e.g., [15]).

II. MERITS OF STUDYING THE AGING OF HARD-SPHERE-LIKE COLLOIDAL SYSTEMS

To study the dynamics of aging, we use 2D and 3D polydisperse hard-sphere-like systems. We chose weakly polydisperse colloidal systems because of the following two reasons. One reason is that, as explained above, we know relevant structural order parameters for them [35,42], which are bond orientational order parameters. In these systems, there is a distinct correlation between an efficient local packing configuration around a particle and the number of its nearest neighbors (6 for two dimensions and 12 for three dimensions), which allows us to characterize the state of packing by a

well-defined structural order parameter. At this moment, it is not possible to have such a simple link between the structure and dynamics for other systems such as binary mixtures of particle with different sizes. This is because for such binary mixtures large fluctuations of the number of nearest-neighbor particles make bond orientational order parameters useless and at this moment we do not know any structural signature responsible for slow dynamics.

Another reason is related to a fundamental importance in the study of aging: The hard-sphere-like systems have significant advantages in elucidating the physical mechanism of glass aging. (i) Only for hard-sphere liquids, we can access the experimental glass transition ($\phi_g \sim 0.58$) by simulations because of the slow microscopic time scale. This allows us to study the aging of a real glass at $\phi = 0.587$ ($> \phi_g = 0.58$) numerically. This is currently impossible for other systems, where we can access only a temperature region far above the *experimentally relevant* glass transition point T_g. (ii) We also emphasize that our previous experimental work [37] indeed confirmed the Ising-like criticality associated with glass transition for polydisperse poly(methyl methacrylate) colloidal systems with a polydispersity of 6% equivalent to our simulations reported in this paper, by confocal microscopy observation. (iii) In aging experiments of other glass-forming liquids such as molecular, polymeric, oxide, and metallic glasses, which are performed under constant pressure, a temperature quench triggering aging inevitably leads to the change not only in the temperature of a sample, but also in its density. Since both of these changes affect glassy dynamics significantly and are coupled with each other, the interpretation of the aging necessarily becomes quite complicated. A pressure jump is a good way to avoid this effect, but it causes adiabatic heating that leads to another complication. For hard-sphere liquids such as colloidal suspensions, on the other hand, we can change the volume fraction (or the density) alone almost instantaneously. Thus the aging takes place without accompanying any further density change. Using this feature as well as a link between the free volume and the free energy, Zargar *et al.* succeeded in measuring the free energy of colloidal liquids directly by using confocal microscopy [57]. Here we follow the kinetics of aging of hard-sphere-like liquids after the density jump by using Brownian dynamics simulations. At $t_w = 0$, we increase the radius of particles, or the volume fraction ϕ, in a preequilibrated liquid, which triggers the aging (see Sec. IV B). This method is similar to recent interesting aging experiments performed by Yunker *et al.* for volume-controllable soft binary colloids [59].

III. CHOICE OF THE RELEVANT ORDER PARAMETER LINKED TO SLOW DYNAMICS

Here we consider what the relevant structural order parameters linked to glassy slow dynamics are for our 2D and 3D polydisperse colloidal systems. We addressed this issue in our previous studies [33–37,42,48] and showed that when the polydispersity is rather small, the relevant order parameter is hexatic order Ψ_6 for two dimensions and Q_6 for three dimensions. We stress that bond orientational order develops simply due to the fact that it is directly linked to the most efficiently packed structure for hard disks and

spheres. A region with higher order has more correlational entropy: Despite the ability of structures with higher bond orientational order to be compacted more efficiently, these structures occupy the same volume as disordered structures in a liquid state. This extra free volume allows the increase of the local correlational (or vibrational) entropy, which is the reason why such structures are favored [42,48]. Note that for hard disks and spheres the free energy is determined by the entropy alone. Since bond orientational order is directly linked with the number of nearest-neighbor particles, it is a relevant order parameter as far as the fluctuations of the number of nearest neighbors due to the particle size polydispersity are rather modest. In our previous studies [32–36], we introduced random disorder and frustration effects to 2D and 3D colloidal systems that have hexatic or Q_6 ordering, respectively, in the absence of such disorder: We systematically increased the strength of the frustration against crystallization and found that a system starts to form glass if the degree of the polydispersity exceeds some critical value and, in a weakly disordered regime, a system preserves the type of order in its pure state. Furthermore, we found that the strength of the frustration against crystallization controls the fragility of a liquid. We confirmed the link between slow structures and the underlying order attained in the absence of the frustration effects, not only for 2D and 3D polydisperse colloidal systems (through simulations [33,35,36] and experiment [37]) but also for 2D driven granular matter [34], 3D Lennard-Jones systems [35], and 2D spin liquids [32] in which the underlying order is antiferromagnetic order, indicating the generality of the link irrespective of the type of order. We also found that the length scale extracted from the order parameter coincides with that of the dynamical correlation in glassy dynamics [32–37]. Furthermore, we confirmed (see, e.g., Fig. 1 of Ref. [35]) that the degree of hexatic order is almost perfectly anticorrelated to the mobility of particles. This supports the validity of our assignment of the structural order parameters responsible for glassy slow dynamics. So, at least in these hard-sphere-like systems, the slowing down of the dynamics is induced by structural ordering linked to Ψ_6 and Q_6.

We note that a bond orientational order parameter is relevant only when fluctuations of the number of nearest-neighbor particles are rather small. Thus, it is not so useful for systems with large polydispersity and binary mixtures of particles with different sizes where the fluctuation of the number of nearest-neighbor particles is inevitably significant [42,48,61]. It is a crucial remaining issue whether or not there is static structural signature linked to slow dynamics even in such systems.

IV. SIMULATION METHODS AND ANALYSES

A. Numerical simulations

Experimentally, a polydisperse colloidal system has often been used as a model glass-forming liquid and the importance of polydispersity in the glass-forming ability has recently been emphasized [37,62,63]. We simulate the behavior of such colloidal systems by using standard Brownian dynamics simulations of polydisperse colloidal particles (disks) interacting with the Weeks-Chandler-Andersen repulsive potential [64]

$U_{ik}(r) = 4\epsilon[(\sigma_{ik}/r)^{12} - (\sigma_{ik}/r)^6 + 1/4]$ for $r < 2^{1/6}\sigma_{ik}$, otherwise $U_{ik}(r) = 0$, where $\sigma_{jk} = (\sigma_{2\mathrm{D}(3\mathrm{D})}^j + \sigma_{2\mathrm{D}(3\mathrm{D})}^k)/2$ and $\sigma_{2\mathrm{D}(3\mathrm{D})}^j$ represents the size of particle j in the 2D (3D) system. We introduce the Gaussian distribution of particle sizes. Its standard deviation is regarded as the polydispersity:

$$\Delta_{2\mathrm{D}(3\mathrm{D})} = \sqrt{\langle(\sigma_{2\mathrm{D}(3\mathrm{D})})^2\rangle - \langle\sigma_{2\mathrm{D}(3\mathrm{D})}\rangle^2}/\langle\sigma_{2\mathrm{D}(3\mathrm{D})}\rangle,$$

where $\langle x \rangle$ means the average of variable x^i. For all simulations, the temperature is fixed at $k_B T/\epsilon = 0.025$ and the particle number is $N_p = 16\,384$. In our previous study [33] we described the phase behavior of this system as a function of Δ and ϕ. A system of smaller polydispersity ($\Delta_{2\mathrm{D}} \leqslant 9\%$ and $\Delta_{3\mathrm{D}} \leqslant 6\%$) (quasi-)long-range ordering emerges upon increasing the packing fraction ($\phi^{2\mathrm{D}}$ for two dimensions and $\phi^{3\mathrm{D}}$ for three dimensions). In our present study we introduce the effective diameter of particle j, d^j, which satisfies the relation $U(d_{2\mathrm{D}(3\mathrm{D})}) = k_B T$. We obtain $d_{2\mathrm{D}(3\mathrm{D})} = 1.0953\sigma_{2\mathrm{D}(3\mathrm{D})}$ as the corresponding hard-sphere diameter. Using these effective diameters, we define the packing fraction of colloids as follows: For two dimensions, $\phi^{2\mathrm{D}} = (1/L_{2\mathrm{D}}^2)\sum_j^{N_p}\pi(d_{2\mathrm{D}}^j/2)^2$, where $L_{2\mathrm{D}}$ is the box size in two dimensions, and for three dimensions, $\phi^{3\mathrm{D}} = (1/6L_{3\mathrm{D}}^3)\sum_j^{N_p}\pi(d_{3\mathrm{D}}^j)^3$, where $L_{3\mathrm{D}}$ is the box size in three dimensions. In a repulsive system, $1/\phi^{2\mathrm{D}(3\mathrm{D})}$ plays the same role as the temperature T in molecular liquids. For larger $\Delta_{2\mathrm{D}(3\mathrm{D})}$, we observe vitrification instead of such (quasi-)long-range ordering [33,35,36]. We used a system with $\Delta_{2\mathrm{D}} = 11\%$ for two dimensions and one with $\Delta_{3\mathrm{D}} = 6\%$ for three dimensions.

B. Method of volume quench

Next we explain how to initiate aging in our numerical simulations. First, we prepare the initial configurations at an equilibrium liquid state, i.e., at $\phi_{\mathrm{ini}}^{2\mathrm{D}} = 0.69$, which is slightly below the hexatic ordering point $\phi_I^{2\mathrm{D}}$ of monodisperse disks ($\Delta_{2\mathrm{D}} = 0$), and at $\phi_{\mathrm{ini}}^{3\mathrm{D}} = 0.48$, which is slightly below the freezing point $\phi_F^{3\mathrm{D}} = 0.494$ of monodisperse hard spheres ($\Delta_{3\mathrm{D}} = 0$). Then we perform a volume jump, or increase the packing fraction ϕ, by increasing the size of each particle with the same ratio while avoiding overlap. For two dimensions, we use three target volume fractions $\phi^{2\mathrm{D}} = 0.756$, 0.772, and 0.784, whereas for three dimensions we use $\phi^{3\mathrm{D}} = 0.550$, 0.568, and 0.587. This volume jump may apparently look similar to the temperature quench in molecular liquids. However, we stress that there is no slow change in the density after the quench in our system, unlike ordinary glass-forming systems such as molecular liquids. We set the waiting time $t_{\mathrm{w}} = 0$ to the time when the volume quench is accomplished. We follow the aging process as a function of t_{w}.

C. Analysis of the dynamics

We calculate the intermediate scattering function (ISF) at t_{w}, $F(q_p,t,t_{\mathrm{w}}) = 1/N_p \sum_{j=1}^{N_p} \exp\{-i\vec{q}_p \cdot [\vec{r}_j(t) - \vec{r}_j(0)]\}$, where q_p is the wave number that corresponds to the first peak of the static structure factor $S(q)$. During aging, we make a fitting of the ISF over a rather narrow time span, which is necessary for making a link between the relaxation dynamics and instantaneous static order over a similar time
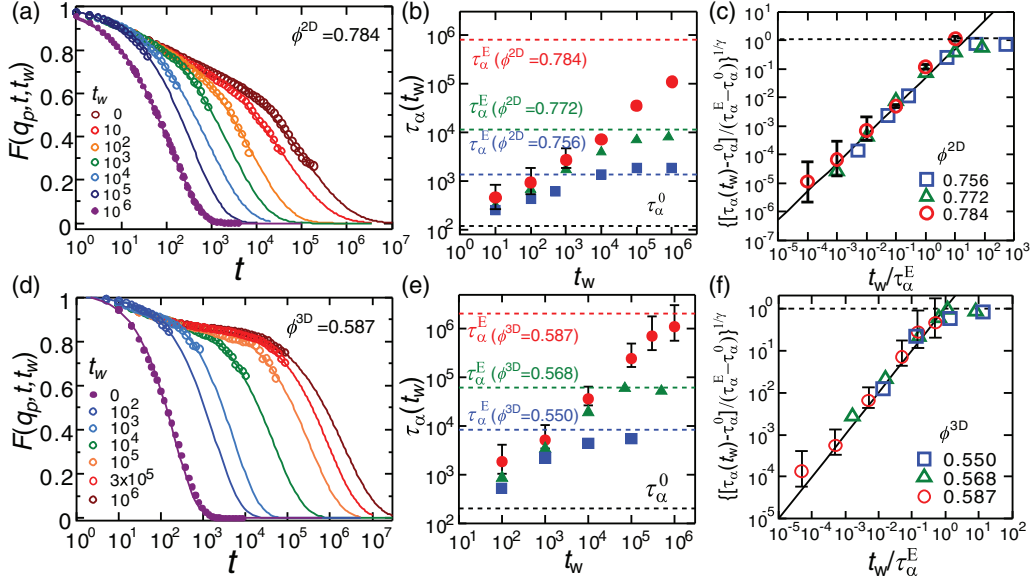
FIG. 1. (Color online) Slowing down of the dynamics during aging for (a)–(c) the 2D systems ($\Delta_{2D} = 11\%$) and (d)–(f) the 3D systems ($\Delta_{3D} = 6\%$). (a) Dependence of $F(q_p, t, t_w)$ on t_w. The solid lines represent the stretched exponential function for $\phi^{2D} = 0.784$. (b) Dependence of τ_α on t_w for $\phi^{2D} = 0.756$, 0.772, and 0.784. Here τ_α^E is the relaxation time of the ergodic state for each ϕ^{2D}, $\tau_\alpha^E = 1.4 \times 10^3$, 1.15×10^4, and 8.2×10^5, respectively, and τ_α^0 is the relaxation time of the initial equilibrium liquid state, $\tau_\alpha^0 = 1.2 \times 10^2$. (c) Dependence of $\{[\tau_\alpha(t_w) - \tau_\alpha^0]/(\tau_\alpha^E - \tau_\alpha^0)\}^{1/\gamma}$ on t_w/τ_α. The solid lines represent the relation $\{[\tau_\alpha(t_w) - \tau_\alpha^0]/(\tau_\alpha^E - \tau_\alpha^0)\}^{1/\gamma} = At_w/\tau_\alpha^E$ with $A = 0.05$. For each ϕ, the relationship between $\tau_\alpha(t_w)$ and t_w is expressed by the same functional form. The power-law exponent γ is 0.30, 0.41, and 0.59 for $\phi^{2D} = 0.756$, 0.772, and 0.784, respectively. (d) Same as (a) for three dimensions ($\phi^{3D} = 0.587$). (e) Same as (b) for three dimensions. Here $\tau_\alpha^E = 7.6 \times 10^3$, 6.2×10^4, and 1.5×10^6 for $\phi^{3D} = 0.550$, 0.568, and 0.587, respectively, and $\tau_\alpha^0 = 2.0 \times 10^2$. (f) Same as (c) for three dimensions. Here $\gamma = 0.75$, 0.77, and 0.80 for $\phi^{3D} = 0.550$, 0.568, and 0.587, respectively, and $A = 1$. We include the error bars for a part of the aging data to show possible errors due to the limited range of the time span used for the analysis of the ISF data.

duration. We fit the ISF by the two-step stretched exponential function (the so-called Kohlrausch-Williams-Watts function) $F(q_p, t, t_w) = (1 - a) \exp[-(t/\tau_\beta)] + a \exp[-(t/\tau_\alpha)^\beta]$, where a is the Debye-Waller factor, τ_β is the fast β relaxation time, τ_α is the α relaxation time, and β is the stretching parameter. In this study we fix the value of β as $\beta = 0.5$ for two dimensions and $\beta = 0.7$ for three dimensions to reduce the number of fitting parameters. These values are chosen on the basis of the analysis of quasiequilibrium results. However, a recent experimental study indicates the increase of β in the early stage of aging [65]. In other words, the scaling of the ISF does not work during aging. Thus, the rather narrow time span and the fixing of β may result in rather large errors. We estimate the amplitude of the errors from fitting the ISFs with the ambiguity of β in the range of ± 0.2: $0.3 \leqslant \beta \leqslant 0.7$ for two dimensions and $0.5 \leqslant \beta \leqslant 0.9$ for three dimensions. The error bars are shown for a part of the aging data in Figs. 1 and 3.

D. Analysis of two-body density correlation

We characterize the structure of a liquid by the radial distribution function $g(r) = 1/\rho N \langle \rho(\vec{r})\rho(\vec{0}) \rangle$, where ρ is the average density and $\rho(\vec{r})$ is the local density at $\vec{r}$.

E. Characterization of bond orientational order

For 2D polydisperse hard disks, we measured a sixfold hexatic bond orientational order parameter [33,34,66] to

characterize the local structural order $\Psi_6^j = |\frac{1}{n_j} \sum_{m=1}^{n_j} e^{i 6\theta_m^j}|$, where n_j is the number of nearest neighbors of particle j, $i = \sqrt{-1}$, and θ_m^j is the angle between $\vec{r}_m - \vec{r}_j$ and the x axis, where particle m is a neighbor of particle j. Note that $\Psi_6^j = 1$ means the perfect hexagonal arrangement of six nearest-neighbor particles around particle j and $\Psi_6^j = 0$ means a random arrangement.

We calculate the spatial correlation function of ψ_6 as $g_6(r)/g(r) = \langle \psi_6(\vec{r})\psi_6^*(\vec{r}) \rangle / g(r)$, where

$$\psi_6(\vec{r}) = \frac{1}{N_p} \sum_{j=1}^{N_p} \frac{1}{n_b} \sum_{m=1}^{n_b} e^{i 6\theta_m^j} \delta(\vec{r} - \vec{r}_j)$$

(n_b being the number of nearest neighbors). We can estimate the correlation length ξ_6 by fitting to the envelope of the correlation function $g_6(r)/g(r)$ the 2D Ornstein-Zernike function $r^{-1/4} \exp[-(r/\xi_6)]$ [see Fig. 4(a)].

For 3D polydisperse colloids, we used the sixth-order bond orientational order parameter for particle k: Q_6^j. The lth-order bond orientational order parameter of particle k is calculated as

$$Q_l^k = \frac{4\pi}{2l + 1} \left(\sum_{m=-l}^{l} |Q_{lm}^k|^2 \right)^{1/2}.$$

Here $Q_{lm}^k = 1/N_b^k \sum_{j=1}^{N_b^k} q_{lm}(\vec{r}_{kj})$, N_b^k is the number of the nearest neighbors of particle k including particle k itself,

and $q_{lm}^k = 1/n_b^k \sum_{j=1}^{n_b^k} Y_{lm}(\vec{r}_{kj})$, where $Y_{lm}(\vec{r}_{kj})$ is a spherical harmonic function of degree l and order m and n_b^k is the number of bonds of particle k. The time average is taken for a period of τ_α. The spatial coarse graining added to the standard Steinhardt bond orientational order parameter [39,67] leads to a significant improvement in detecting the structural order [68].

The correlation function of this structural order can be calculated as

$$g_6^{3D}(r)/g(r) = \frac{4\pi}{13}\left\langle\sum_{m=-6}^{6} Q_{6m}(\vec{r})Q_{6m}^*(\vec{0})\right\rangle \bigg/ g(r).$$

Then we can obtain the correlation length by fitting the the following 3D Ornstein-Zernike function to the envelope of this correlation function: $g_6^{3D}(r)/g(r) \propto r^{-1}\exp(-r/\xi_6)$ [see Fig. 4(d)].

V. RESULTS AND DISCUSSION

A. Aging in 2D polydisperse colloids

1. Dynamical slowing down during aging

First we focus on the aging dynamics in 2D systems. To see the slowing down of the structural relaxation during aging,

we calculate the intermediate scattering function $F(q_p,t,t_w)$ as a function of t_w. The results are shown in Fig. 1(a). We take a rather narrow time span of the ISF for making a link between the relaxation dynamics and instantaneous static order over a similar time duration, although this causes errors in the estimation of τ_α. By fitting the stretched exponential function for a time regime of $t \lesssim t_w$, we estimate the structural relaxation time τ_α as a function of t_w, whose results are shown in Fig. 1(b). We confirm that τ_α monotonically increases with t_w and eventually saturates around $t_w = 30\tau_\alpha^E$ toward its ergodic value τ_α^E, which was determined by (quasi)equilibrium simulations. Here we note that the relaxation of a glass toward its quasiequilibrium supercooled state was also suggested by experiments [69]. In each system of different ϕ^{2D}, the relationship between τ_α and t_w can be commonly described by the function form $[\tau_\alpha(t_w) - \tau_\alpha^0]/(\tau_\alpha^E - \tau_\alpha^0) = A(t_w/\tau_\alpha^E)^\gamma$, where A and γ are the adjustable parameters [see Fig. 1(c)]. Such a power-law behavior has been known to describe well aging dynamics in spin-glass models [13] and colloidal systems [12].

2. Structural evolution during aging

Next we seek a structural signature of aging. First we show the temporal change of the radial distribution function $g(r)$,
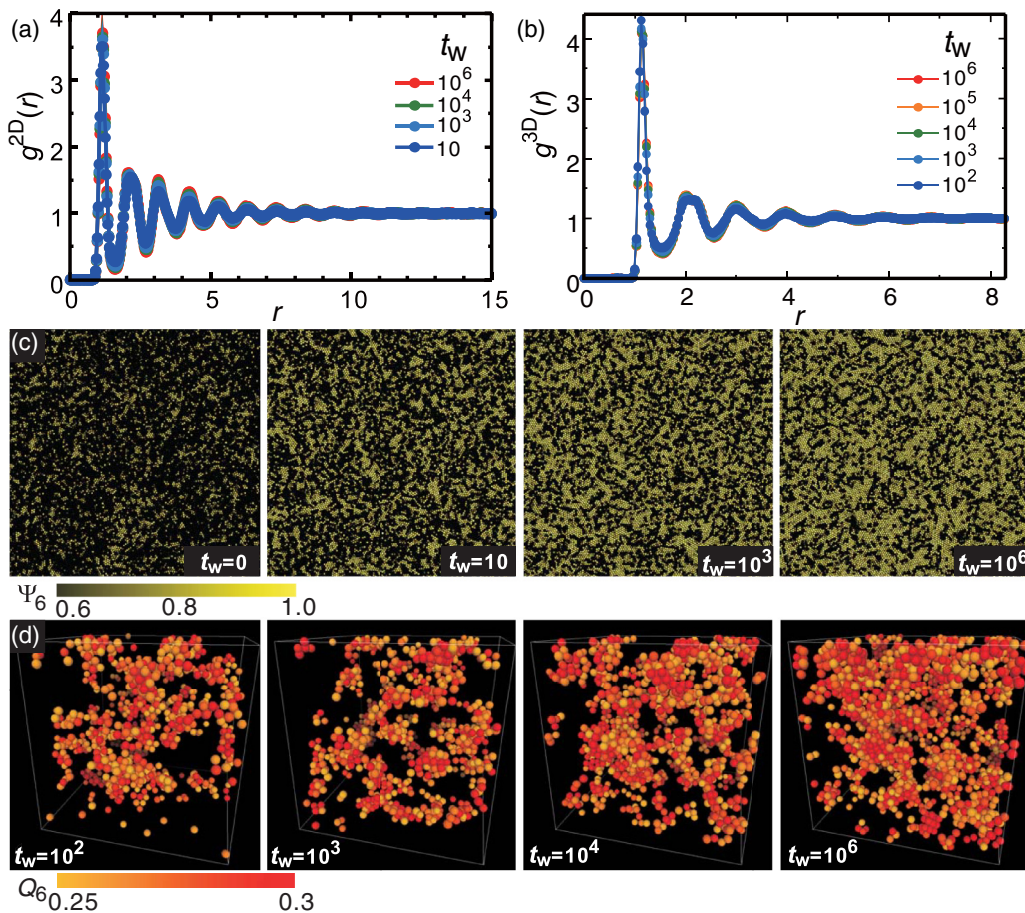

FIG. 2. (Color online) (a) Temporal change in $g(r)$ for the 2D system. (b) Same as (a) but for the 3D system. (c) Structural order in the 2D system ($\phi^{2D} = 0.784$) at t_w=0, 10, 10^3, and 10^6. The colors of the particles represent the values of Ψ_6^j (see the color bar). (d) Structural order in the 3D system ($\phi^{3D} = 0.587$) at $t_w = 10^2$, 10^3, 10^4, and 10^6. Only particles of $Q_6^j > 0.25$ are displayed. The colors of the particles represent the values of Q_6^j (see the color bar).

which is a two-body density correlation, during aging. As can be seen in Fig. 2(a), there is little temporal change in $g(r)$, indicating the absence of translational ordering during aging, i.e., the absence of crystallization in our systems. The exponential decay of $g(r)$ clearly indicates the absence of translational ordering. However, this does not necessarily imply the absence of any structural change. Figure 2(c) shows the structural evolution of hexatic order during aging. We can clearly see that the characteristic size of clusters of particles with high hexatic order (more precisely, the correlation length of hexatic order parameter Ψ_6) ξ_6 grows with an increase in t_w, suggestive of an important role of the growing static correlation in the dynamical slowing down during aging shown in Fig. 1. From our previous study [33–36] we know that for small ϕ^{2D}, almost all particles are in a disordered state, whereas with an increase in ϕ^{2D} the system exhibits slower dynamics, accompanying the increase in both the degree of hexatic order Ψ_6 and its spatial coherence length ξ_6: Long-lived clusters of particles with larger Ψ_6 grow in size and particles in larger clusters are slower in their dynamics. Thus, the process of aging looks like the equilibration process of critical-like fluctuations of hexatic order after a quench. We stress that the process is not like droplet coarsening below the critical point but growth of temporally fluctuating static order above it and thus no noticeable fractionation takes place during aging.

Structural evolution during aging can also be revealed by the temporal change in the number of geometric defects. Geometric defects, or voids, are detected by applying Delaunay triangulation [35], as shown in Fig. 3. Defects are defined as follows [35,70]. If the distance between two neighboring particles j and m satisfies $r_{jm} < c \times (d_{2D}^j + d_{2D}^m)/2$ with $c = 1.4$, we regard them as being connected; otherwise we cut the bond. When a bond is cut, the two triangles sharing it become a square. Any polygons besides triangles are regarded as voids, which appear as holes in Fig. 3(a).

In the initial stage (at $t_w = 10^2$), there are many geometric defects that are mostly squares ($N = 4$) (N being the number of the sides of a polygon). In the late stage (at $t_w = 10^6$), on the other hand, the number of geometric defects decreases, accompanying the development of hexatic order characterized by triangular tiling. This trend can be more quantitatively seen in the temporal change in the distribution function of N, $P(N)$ [see Fig. 3(b)]. We confirm that with an increase in t_w, $P(3)$ increases as a consequence of the decrease of $P(4)$ [note that $P(3) + P(4)$ is almost constant with time]. This clearly indicates that aging accompanies structural ordering, or the decrease in the number density of defects or voids, which lowers particle mobility.

Next we characterize the spatial correlation length of glassy structural order to make its link to the dynamics more quantitative. Figure 4(a) shows the temporal change in $g_6^{2D}(r)/g(r)$ during aging for $\phi^{2D} = 0.784$. The envelope of the correlation function $g_6^{2D}(r)/g(r)$ is fitted well by the Ornstein-Zernike function, as shown in Fig. 4(a). We show the temporal change in the correlation length ξ_6 in Fig. 4(b), clearly indicating the monotonic increase of ξ_6 with an increase in t_w. We emphasize that such a structural change cannot be seen by two-body correlations [see Fig. 2(a)] and we need many-body correlations to detect it [47].
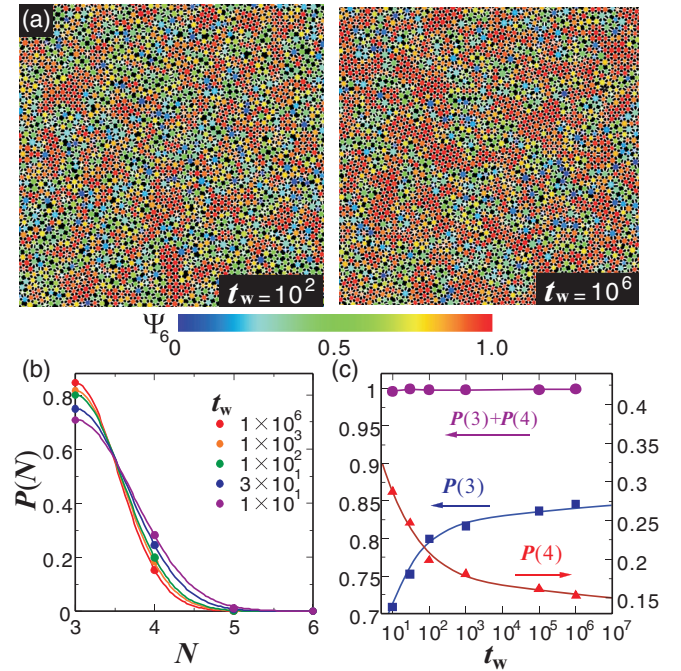

FIG. 3. (Color online) Nature of structural change during aging. (a) Bond patterns at $t_w = 10^2$ and 10^6. Bonds are connected when the interparticle distance r_{jk} satisfies $r_{jk} < c(d_{2D}^j + d_{2D}^k)/2$. The colors of the particles represent the values of the Ψ_6^j (see the color bar). We can see that voids (black vacancies) are located specifically in less ordered regions. With an increase in t_w, the characteristic size of clusters of red particles monotonically increases. (b) Dependence of the distribution function of the number of sides of polygons N, $P(N)$, on t_w. We can see geometric defects, or voids, which are characterized as polygons with $N \geqslant 4$. (c) Dependence of $P(3)$, $P(4)$, and $P(3) + P(4)$ on t_w. We confirm that as t_w increases, $P(4)$ deceases whereas $P(3)$ increases [note that $P(3) + P(4)$ is almost equal to 1 and constant with time]. This indicates that the number of triangles $P(3)$ increases at the expense of geometric defects of square type $P(4)$, leading to the growth of hexatic order with the aging time, which can clearly be seen in (a) and (b).

3. Structure-dynamics correlation during aging

Now we seek a relationship between ξ_6 and τ_α during aging. For an ergodic supercooled liquid state of the same system, we found the following phenomenological relations [33]:

$$\tau_\alpha = \tau_0 \exp[D(\xi_6/\xi_{60})^{d/2}], \quad (1)$$

$$\xi_6 = \xi_{60}[(\phi_0 - \phi)/\phi]^{-\nu}, \quad (2)$$

where d is the spatial dimensionality, τ_0 is the microscopic time scale, D is the fragility index (the larger D means that a liquid is less fragile, or stronger [4]), ξ_{60} is the bare correlation length, and ν is the Ising exponent for the correlation length ($\nu \cong 2/d$) [60]. Equation (1) implies that the slowing down is a consequence of the growth of the correlation length upon densification. This relation may be characteristic of critical phenomena of a system suffering from frustration [35,42,51–53]. In our systems, the frustration is due to the size polydispersity of particles Δ, which induces
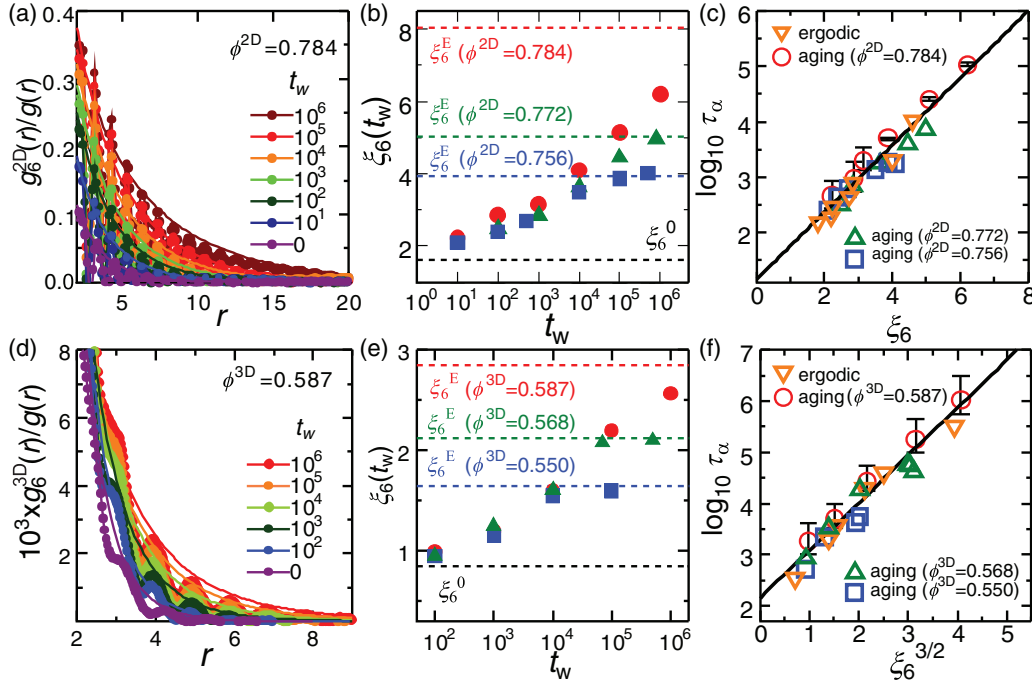
FIG. 4. (Color online) Growing correlation length during aging and its link to the slowing down of the dynamics. (a) Dependence of $g_6^{2D}(r)/g(r)$ on t_w for $\phi^{2D} = 0.784$. The solid lines are the Ornstein-Zernike function $g_6^{2D}(r)/g(r) \propto r^{-1/4} \exp[-(r/\xi_6)]$. (b) Growth of ξ_6 with t_w for $\phi^{2D} = 0.756$, 0.772, and 0.784. Here ξ_6^E is the correlation length of the final ergodic state, $\xi_6^E = 3.95$, 5.02, and 8.05 for $\phi^{2D} = 0.756$, 0.772, and 0.784, respectively, and ξ_6^0 is the correlation length at the initial state and common to the different final values of ϕ^{2D}. (c) Relationship of τ_α to ξ_6 during the aging process of the 2D systems ($\Delta_{2D} = 11\%$) for $\phi^{2D} = 0.756$, 0.772, and 0.756. The relation for the ergodic system is also shown for the same system of $\Delta = 11\%$ [33] (here the particle number $N_p = 16\,384$). The solid line represents $\tau_\alpha = \tau_0 \exp(D\xi_6/\xi_{60})$, which is confirmed for an ergodic system [33] with $D = 0.35$, $\xi_{60} = 0.25$, and $\tau_0 = 14.1$. (d) Same as (a) for three dimensions ($\phi^{3D} = 0.587$). (e) Same as (b) for three dimensions. Here $\xi_6^E = 1.65$, 2.12, and 2.85 for $\phi^{3D} = 0.550$, 0.568, and 0.587, respectively, and $\xi_6^0 = 0.85$. (f) Relationship of τ_α to ξ_6 during the aging process of the 3D systems ($\Delta_{3D} = 6\%$) for $\phi^{3D} = 0.550$, 0.568, and 0.587. The parameters are $D = 0.72$, $\xi_{60} = 0.51$, and $\tau_0 = 107.2$, which are determined for the ergodic liquid [35]. We include the error bar for a part of the aging data (see the caption of Fig. 1).

frustration effects on crystallization [42,48]. The results shown in Fig. 4(c) suggest that the same relation between the two quantities [Eq. (1)] holds for both quasiequilibrium and nonequilibrium states with the common parameters (τ_0, ξ_{60}, D, ϕ_0, and ν), which is remarkable.

B. Aging in 3D polydisperse colloids

We also examine whether the above findings are also relevant to a 3D polydisperse hard-sphere-like colloidal system, which is one of the ideal glass formers [71]. Figures 1(d)–1(f) show the dynamical slowing down during aging and the basic features are the same as those of the 2D system. Although there is little change in $g(r)$ as shown in Fig. 2(b), we can clearly see the temporal evolution of crystal-like bond order parameter in Fig. 2(d), similarly to the case of the 2D system. The quantitative analysis of the spatial correlation of the bond order parameter tells us that the correlation length $\xi_6(t_w)$ monotonically increases with an increase in t_w [see Fig. 4(e)]. We also confirm that the relation between ξ_6 and τ_α [Eq. (1) with $d = 3$] also holds not only for the quasiequilibrium ergodic supercooled liquid but also for the aging process [see Fig. 4(f)]. These results strongly suggest the generality of this connection between the static correlation length and the dynamics at least for polydisperse colloidal

systems, irrespective of the spatial dimensionality ($d = 2$ and 3).

VI. SUMMARY

This link between the correlation length of the static structural order and the dynamics has a remarkable message that the slow dynamics of both supercooled liquids (in metastable equilibrium) and aging glasses (out of equilibrium) can be described on the same ground and is controlled solely by the degree of critical-like fluctuations of a glassy structural order parameter, which may have a one-to-one connection to the free energy of the system. This looks consistent with the argument that the aging dynamics follows the statistics of the system in equilibrium [6]. The state of supercooled liquids and glasses may thus be characterized by a single quantity, the correlation length of glassy structural order, which can be regarded as a measure of the age of a glass. Furthermore, this scenario implies that aging effects are more significant in a more fragile glass former, which exhibits a steeper increase in the correlation length with increasing ϕ.

We emphasize that the volume fraction ϕ is kept constant (see Sec. II) and the two-body density correlator exhibits little change throughout the process of aging for our systems. For example, the latter suggests that the behavior is difficult to

explain by the mode-coupling theory (see also [49] for a similar conclusion for an equilibrium case). We argue that the slowing down of the dynamics is primarily induced by the growth of critical-like fluctuations of crystal-like bond orientational order. Here we stress that crystal-like bond orientational order should not be confused with crystal order accompanying translational order. A region of high orientational order still has large fluctuations of interparticle distance and thus no translational order, which is supported by the behavior of $g(r)$ in Figs. 2(a) and 2(b) (see also [37,48]). On noting that particles with higher order are statistically slower [33–37], the glassy slow dynamics in our systems is thought to be the consequence of the growing structural correlation. This is reminiscent of the dynamical scaling in critical phenomena [42]: The growth of glassy structural ordering during aging may be regarded as an analog of the time evolution of critical fluctuations in the Ising magnets after a temperature jump toward the critical point within the paramagnetic region, yet frustration leads to the activation-type critical dynamics [35,42,48,51–53], which may be responsible for the extremely slow growth kinetics of order parameter fluctuations. Thus, this implies not only the validity of the dynamical scaling in glass aging but also an intimate link between the glass transition and critical phenomena. It is remarkable that the link between the glass transition and critical phenomena is supported not only by the equilibrium static aspect [35] but also by the out-of-equilibrium dynamical aspect. We also note that both the length and time scale of aging can be scaled by their final equilibrium values ξ_6^E and τ_α^E,

respectively, as in the case of the dynamical scaling in critical phenomena.

Aging of glasses progresses through a sequence of quasiequilibrium thermalization of the configurational degrees of freedom, which are characterized by bond orientational order in our systems. This implies that in our systems the effective temperature of an out-of-equilibrium state [13,16] has a direct link to the correlation length of bond orientational order fluctuations. However, bond orientational order is valid only for quasi-one-component systems (see Sec. III) such as polydisperse hard spheres studied here, but not, e.g., for binary systems [42,45,48,61]. Thus, the generality of the above statement needs to be checked carefully in the future. We speculate that bond orientational order may be rephrased as low-free-energy configurations in a more general perspective [42]. In relation to this, a link of our scenario to a more general scenario such as the Adam-Gibbs theory [72–74] is an interesting issue, since our structural order is correlated with the local configurational entropy.

ACKNOWLEDGMENTS

[1] A. Cavagna, Phys. Rep. **476**, 51 (2009).

[2] L. Berthier and G. Biroli, Rev. Mod. Phys. **83**, 587 (2011).

[3] R. C. Welch, J. R. Smith, M. Potuzak, X. Guo, B. F. Bowden, T. J. Kiczenski, D. C. Allan, E. A. King, A. J. Ellison, and J. C. Mauro, Phys. Rev. Lett. **110**, 265901 (2013).

[4] C. A. Angell, K. L. Ngai, G. B. McKenna, P. F. McMillan, and S. W. Martin, J. Appl. Phys. **88**, 3113 (2000).

[5] W. Kob and J. L. Barrat, Phys. Rev. Lett. **78**, 4581 (1997).

[6] W. Kob, F. Sciortino, and P. Tartaglia, Europhys. Lett. **49**, 590 (2000).

[7] S. M. Fielding, P. Sollich, and M. E. Cates, J. Rheol. **44**, 323 (2000).

[8] B. Abou and F. Gallet, Phys. Rev. Lett. **93**, 160603 (2004).

[9] P. Wang, C. Song, and H. A. Makse, Nat. Phys. **2**, 526 (2006).

[10] S. Jabbari-Farouji, D. Mizuno, M. Atakhorrami, F. C. MacKintosh, C. F. Schmidt, E. Eiser, G. H. Wegdam, and D. Bonn, Phys. Rev. Lett. **98**, 108302 (2007).

[11] J. M. Lynch, G. C. Cianci, and E. R. Weeks, Phys. Rev. E **78**, 031410 (2008).

[12] M. Bellour, A. Knaebel, J. L. Harden, F. Lequeux, and J.-P. Munch, Phys. Rev. E **67**, 031405 (2003).

[13] J. P. Bouchaud, L. F. Cugliandolo, J. Kurchan, and M. Mézard, in *Spin Glasses and Random Fields*, edited by A. P. Young, Series on Directions in Condensed Matter Physics Vol. 12 (World Scientific, Singapore, 1998).

[14] E. Vincent, J. Hammann, M. Ocio, J.-P. Bouchaud, and L. Cugliandolo, in *Complex Behaviour of Glassy Systems*, edited

by M. Rubi, Lecture Notes in Physics Vol. 492 (Springer, Berlin, 1997), pp. 184–219.

[15] F. Corberi, L. F. Cugliandolo, and H. Yoshino, *Dynamical Heterogeneities in Glasses, Colloids and Granular Media*, edited by L. Berthier, G. Biroli, J.-P. Bouchaud, L. Cipelletti, and W. van Saarloos, International Series of Monographs on Physics Vol. 150 (Oxford University Press, Oxford, 2011), p. 370.

[16] L. F. Cugliandolo, J. Kurchan, and L. Peliti, Phys. Rev. E **55**, 3898 (1997).

[17] G. Parisi, J. Phys. Chem. B **103**, 4128 (1999).

[18] A. Parsaeian and H. E. Castillo, Phys. Rev. E **78**, 060105 (2008).

[19] P. W. Anderson, Science **267**, 1615 (1995).

[20] K. Binder and W. Kob, *Glassy Materials and Disordered Solids: An Introduction to Their Statistical Mechanics* (World Scientific, Singapore, 2011).

[21] M. Foley and P. Harrowell, J. Chem. Phys. **98**, 5069 (1993).

[22] M. M. Hurley and P. Harrowell, Phys. Rev. E **52**, 1694 (1995).

[23] W. K. Kegel and A. van Blaaderen, Science **287**, 290 (2000).

[24] R. Yamamoto and A. Onuki, J. Phys. Soc. Jpn. **66**, 2545 (1997).

[25] W. Kob, C. Donati, S. J. Plimpton, P. H. Poole, and S. C. Glotzer, Phys. Rev. Lett. **79**, 2827 (1997).

[26] E. R. Weeks, J. C. Crocker, A. C. Levitt, A. Schofield, and D. A. Weitz, Science **287**, 627 (2000).

[27] L. Berthier, G. Biroli, J.-P. Bouchaud, L. Cipelletti, and W. van Saarloos, *Dynamical Heterogeneities in Glasses, Colloids, and Granular Media* (Oxford University Press, Oxford, 2011).

[28] R. Yamamoto and A. Onuki, Phys. Rev. E **58**, 3515 (1998).

[29] T. M. Truskett, S. Torquato, S. Sastry, P. G. Debenedetti, and F. H. Stillinger, Phys. Rev. E **58**, 3083 (1998).

[30] A. Widmer-Cooper and P. Harrowell, Phys. Rev. Lett. **96**, 185701 (2006).

[31] G. S. Matharoo, M. S. G. Razul, and P. H. Poole, Phys. Rev. E **74**, 050502(R) (2006).

[32] H. Shintani and H. Tanaka, Nat. Phys. **2**, 200 (2006).

[33] T. Kawasaki, T. Araki, and H. Tanaka, Phys. Rev. Lett. **99**, 215701 (2007).

[34] K. Watanabe and H. Tanaka, Phys. Rev. Lett. **100**, 158002 (2008).

[35] H. Tanaka, T. Kawasaki, H. Shintani, and K. Watanabe, Nat. Mater. **9**, 324 (2010).

[36] T. Kawasaki and H. Tanaka, J. Phys.: Condens. Matter **22**, 232102 (2010).

[37] M. Leocmach and H. Tanaka, Nat. Commun. **3**, 974 (2012).

[38] D. Coslovich, Phys. Rev. E **83**, 051505 (2011).

[39] P. J. Steinhardt, D. R. Nelson, and M. Ronchetti, Phys. Rev. B **28**, 784 (1983).

[40] G. Tarjus, S. A. Kivelson, Z. Nussinov, and P. Viot, J. Phys.: Condens. Matter **17**, R1143 (2005).

[41] V. Lubchenko and P. G. Wolynes, Annu. Rev. Phys. Chem. **58**, 235 (2007).

[42] H. Tanaka, Eur. Phys. J. E **35**, 113 (2012).

[43] G. Biroli, J. P. Bouchaud, A. Cavagna, T. S. Grigera, and P. Verrocchio, Nat. Phys. **4**, 771 (2008).

[44] L. Berthier and W. Kob, Phys. Rev. E **85**, 011102 (2012).

[45] B. Charbonneau, P. Charbonneau, and G. Tarjus, Phys. Rev. Lett. **108**, 035701 (2012).

[46] T. R. Kirkpatrick, D. Thirumalai, and P. G. Wolynes, Phys. Rev. A **40**, 1045 (1989).

[47] M. Leocmach, J. Russo, and H. Tanaka, J. Chem. Phys. **138**, 12A536 (2013).

[48] H. Tanaka, Faraday Discuss. **167**, 9 (2013).

[49] L. Berthier and G. Tarjus, Eur. Phys. J. E **34**, 1 (2011).

[50] D. Coslovich, J. Chem. Phys. **138**, 12A539 (2013).

[51] D. S. Fisher, J. Appl. Phys. **61**, 3672 (1987).

[52] J. S. Langer, Phys. Rev. E **88**, 012122 (2013).

[53] J. S. Langer, Rep. Prog. Phys. **77**, 042501 (2014).

[54] L. Assoud, F. Ebert, P. Keim, R. Messina, G. Maret, and H. Löwen, J. Phys.: Condens. Matter **21**, 464114 (2009).

[55] P. G. Debenedetti and F. H. Stillinger, Nature (London) **410**, 259 (2001).

[56] C. A. Angell, Science **267**, 1924 (1995).

[57] R. Zargar, B. Nienhuis, P. Schall, and D. Bonn, Phys. Rev. Lett. **110**, 258301 (2013).

[58] D. R. Nelson, *Defects and Geometry in Condensed Matter Physics* (Cambridge University Press, Cambridge, 2002).

[59] P. Yunker, Z. Zhang, K. B. Aptowicz, and A. G. Yodh, Phys. Rev. Lett. **103**, 115701 (2009).

[60] A. Onuki, *Phase Transition Dynamics* (Cambridge University Press, Cambridge, 2002).

[61] D. N. Perera and P. Harrowell, J. Chem. Phys. **111**, 5441 (1999).

[62] E. Dickinson, R. Parker, and M. Lal, Chem. Phys. Lett. **79**, 578 (1981).

[63] S. I. Henderson, T. C. Mortensen, S. M. Underwood, and W. van Megen, Physica A **233**, 102 (1996).

[64] J. D. Weeks, D. Chandler, and H. C. Andersen, J. Chem. Phys. **54**, 5237 (1971).

[65] B. Ruta, G. Baldi, Y. Monaco, and G. Chushkin, J. Chem. Phys. **138**, 054508 (2013).

[66] S. E. Abraham, S. M. Bhattacharrya, and B. Bagchi, Phys. Rev. Lett. **100**, 167801 (2008).

[67] P. R. ten Wolde, M. J. Ruiz-Montero, and D. Frenkel, Phys. Rev. Lett. **75**, 2714 (1995).

[68] W. Lechner and C. Dellago, J. Chem. Phys. **129**, 114707 (2008).

[69] P. Lunkenheimer, R. Wehn, U. Schneider, and A. Loidl, Phys. Rev. Lett. **95**, 055702 (2005).

[70] M. A. Glaser and N. A. Clark, Adv. Chem. Phys. **83**, 543 (1993).

[71] P. N. Pusey and W. Van Megen, Nature (London) **320**, 340 (1986).

[72] G. Adam and J. H. Gibbs, J. Chem. Phys. **43**, 139 (1965).

[73] S. Karmakar, C. Dasgupta, and S. Sastry, Proc. Natl. Acad. Sci. U.S.A. **106**, 3675 (2009).

[74] F. W. Starr, J. F. Douglas, and S. Sastry, J. Chem. Phys. **138**, 12A541 (2013).